# SEEPAGE FLOW TEST IN FULL-SCALE EMBANKMENT: SIGNIFICANCE OF L-SHAPED GEOSYNTHETIC DRAIN

**K. Hara[1], S. Shibuya[2], M. Saito[3] & N. Torii[4]**

[1] *Technical Research Center, Taiyokogyo Corporation (Sun), Osaka, Japan. (e-mail: hk002996@mb.taiyokogyo.co.jp)*
[2] *Professor, Department of Civil Engineering, Kobe University, Japan. (e-mail: sshibuya@kobe-u.ac.jp)*
[3] *Assistant Professor, Research Center for Urban Safety and Security, Kobe University, Japan. (e-mail: msaito@kobe-u.ac.jp)*
[4] *Assistant Professor, Research Center for Urban Safety and Security, Kobe University, Japan. (e-mail: torii@kobe-u.ac.jp)*

**Abstract:** Geotechnical engineers in Japan are increasingly concerned with embankment failures induced by heavy rainfalls or earthquakes. In recent earthquakes that occurred in Japan, embankments involved with high water levels were severely damaged, whereas those without seepage water were undamaged. In an attempt to reduce the risk for such embankment failures, Shibuya *et al.* (2008) have recently proposed an L-shaped geodrain system with which seepage water flow into the embankment may be prevented even in the event of heavy rainfalls. In this paper, the results of seepage flow test in full-scale (and fully-instrumented) embankments protected and unprotected by the L-shaped geosynthetic drain are discussed by showing the results of numerical simulation of seepage flow. It was successfully demonstrated that the L-shaped geosynthetic drain was highly effective in preventing seepage flow into the embankment, and also in avoiding the accumulation of water behind it, hence, in reducing the risk for embankment failures associated with heavy rainfalls and/or earthquakes.

**Keywords:** embankment, drainage, geosynthetic, full-scale test, numerical, analysis

## INTRODUCTION

Embankment is usually made of unsaturated soil. Unsaturated soil when properly compacted is stiff and strong, since it sustains the capillary pressure or the matrix suction. The matrix suction disappears quickly in the process of wetting, which in turn may bring about large deformation or even failure of the embankment. A catastrophic failure of Terr Armée wall reported recently by Shibuya *et al.* (2007) was induced by seepage water flow in the event of heavy rainfall, which in turn weakened the fill material by saturation and also pushed the wall by the accumulated water pressure behind the wall. Based on this unique experience, the use of an L-shaped geosynthetic drain comprising a set of vertical and horizontal geosynthetics in the embankment has been proposed by Shibuya *at al.* (2008). Saito *et al.* (2008) has performed numerical simulation in which the efficiency of the L-shaped geodrain system in preventing seepage water flow into the fill was successfully demonstrated. Simultaneously, Hara *et al.* (2007, 2008) examined transmissivity of two types of geosynthetics, i.e., non-woven geotextiles and plastic board drains (PBD), suggesting that the type of geosynthetics having a stiff core material such as PBD is superior to non-woven geotextiles since the in-soil transmissivity of the PBD was scarcely deteriorated due to the sustained pressure.

Seepage flow test using a full-scale test embankment (3.9m in length, 2.0m in width and 2.5m in height) made by means of compaction using a well-graded decomposed granite soil was carried out in this study. The behaviour of the test embankment undertaking seepage flow from the back was carefully examined by monitoring settlement, lateral deformation, pore pressures and moisture content at several points in the test embankment. The efficiency of the L-shaped geosynthetic drain was examined by performing two tests with and without the L-shaped geosynthetic drain. Numerical analysis was also performed in order to simulate the seepage flow characteristics in the unsaturated embankment.

## OUTLINE OF NUMERICAL SIMULATION

The numerical simulation has been described in detail by Saito *et al.* (2008). In the numerical analysis, the following Richards' equation (Richards, 1931) is employed as the governing equation;

$$\left(C+\beta S_s\right)\frac{\partial \psi}{\partial \mathrm{t}}=\nabla\cdot\left[\mathbf{K}\cdot\left(\nabla\psi+\nabla Z\right)\right] \qquad (1)$$

where $C$ is the specific water capacity ($=\phi \mathrm{d}S_w/\mathrm{d}\psi$) (n.b., $\phi$: porosity, and $S_w$: the degree of saturation($0\le S_w\le 1$)), $S_s$ is the specific storage coefficient, K is the hydraulic conductivity tensor, $\psi$ is the pressure head, and Z is the elevation head. Note that $\beta$ is equal to unity in the saturated zone involved with $S_w = 1$, and to zero in the unsaturated zone with $S_w \neq 1$. The K can be expressed in terms of the relative permeability $k_r$ and the saturated hydraulic conductivity $K_s$, that is;

$$\mathbf{K} = k_r \cdot \mathbf{Ks} \qquad (2)$$

The boundary condition on $\Gamma_1$, where the pore pressure head is defined, is given by

$$\psi = \psi_1 \quad \text{on} \quad \Gamma_1 \tag{3}$$

On the boundary $\Gamma_2$, the flux $q$ is defined in the following form;

$$q = q_2 = -\mathbf{n} \cdot \mathbf{K} \cdot (\nabla \psi + \nabla Z) \quad on \quad \Gamma_2 \tag{4}$$

where **n** denotes the outwardly directed unit normal vector.

The relative permeability $k_r$ is an essential parameter in the seepage analysis. This property is considered as a function of $S_w$, whereas $S_w$ is considered as a function of capillary pressure $\psi_c$ ($\equiv -\psi$). Among many mathematical models previously proposed to describe the water retention curve, the van Genuchten equation (van Genuchten, 1980) (i.e., VG model) is employed in the present study; i.e.,

$$S_e = \frac{S_w - S_r}{S_f - S_r} = \left\{1 + (\alpha \psi_c)^n\right\}^{-m} \tag{5}$$

where $S_e$ is the effective saturation, $S_r$ is the residual saturation, $S_f$ is the saturation at $\psi_c$ =0, and $\alpha$, $n$ and $m$ are parameters. The parameters, $n$ and $m$, are both dimensionless, whereas α has the dimension that can be defined as the reciprocal of the pressure head. The parameters $n$ and $m$ are not independent to each other, and they are related by

$$m = 1 - 1/n \tag{6}$$

The relative permeability and effective saturation are interrelated as shown in the following form (Maulem, 1976);

$$k_r = S_e^{\varepsilon} \left\{1 - \left(1 - S_e^{1/m}\right)^m\right\}^2 \tag{7}$$

where $\varepsilon$ is a parameter regarding the degree of interconnection among voids. Generally, a value of 0.5 is used for $\varepsilon$. The water retention curve and relative permeability can be calculated when the parameters $\alpha$, $n$, $S_r$ and $S_f$ are all given.

The relationship between the degree of saturation $S_w$ and the capillary pressure $\psi_c$ exhibits a hysteretic curve against cycles of wetting and drying. In this study, the $\alpha$, $n$, $S_r$ and $S_f$ were all identified by fitting the measured drying curve. In simulating the wetting curve, $\alpha$ was doubled in value while the values of $n$, $S_r$ and $S_f$ remained all constant (refer to Luckner *et al*., 1989). It should be mentioned that the technique proposed by Scott *et al*. (1983) was used for estimating the scanning curves to describe the hysteretic water retention characteristics (for details, refer to Saito *et al.*, 2008).

## FULL-SCALE TEST

### Full-scale embankment

The test embankment had dimensions of 2.5m in height, 2.0m in width and 3.9m in length. It was made by using a total amount of approximately 20m$^3$ of decomposed granite soil having a mean particle diameter of 1.15mm, and a maximum dry density of 1.938g/cm$^3$ with an optimum water content of 11.6% (for details, see Saito *et al.*, 2008). The embankment was constructed in stages, each in which the prescribed amount of the air-dried soil having the initial water content of 8% on average was compacted to form a 0.25m thick layer.

A couple of comparative tests with and without L-shaped geosynthetic drain, these called hereafter case 1 and case 2, respectively, were performed. Figures 1 and 2 show the configuration of these two embankments. The dry density was about 85% and nearly 90% of the maximum dry density for case 1 and case 2, respectively. It should be mentioned that in case 2 embankment with L-shaped geosynthetic drain, the compaction of the upstream portion facing the water supply pipes was not straightforward owing to the limited working space so that the degree of compaction was about 86%, which was lower than the downstream portion with the compaction of nearly 90%.

In both the cases, the seepage flow was initiated by raising the water level in the water supply pipes installed at one end of the embankment. The other end was reinforced by using five rectangular-shaped EPS blocks, each wrapped with a sheet of geogrid. It should be mentioned that the EPS blocks were light in weight, and not connected to each other. Accordingly, the wall facing was rather considered flexible. In case 2 embankment, a set of geosynthetic sheets comprising a 11mm thick core material covered with non-woven geotextiles jacket was installed vertically and horizontally to form the L-shape drain.

Figure 3 shows instrumentation used for monitoring the behaviour of the embankment during the seepage test. The deformation was measured with the settlement plates and the inclinometers for the vertical and horizontal deformation, respectively. An inclinometer made of a PVC pipe was fixed at the bottom. It comprised a set of strain gauges mounted every 0.25m along the vertical to measure the deflection of the pipe. The number of inclinometers installed was four and three for case 1 and case 2, respectively. The seepage water level in the embankment was continuously monitored at three positions by using stand pipes.

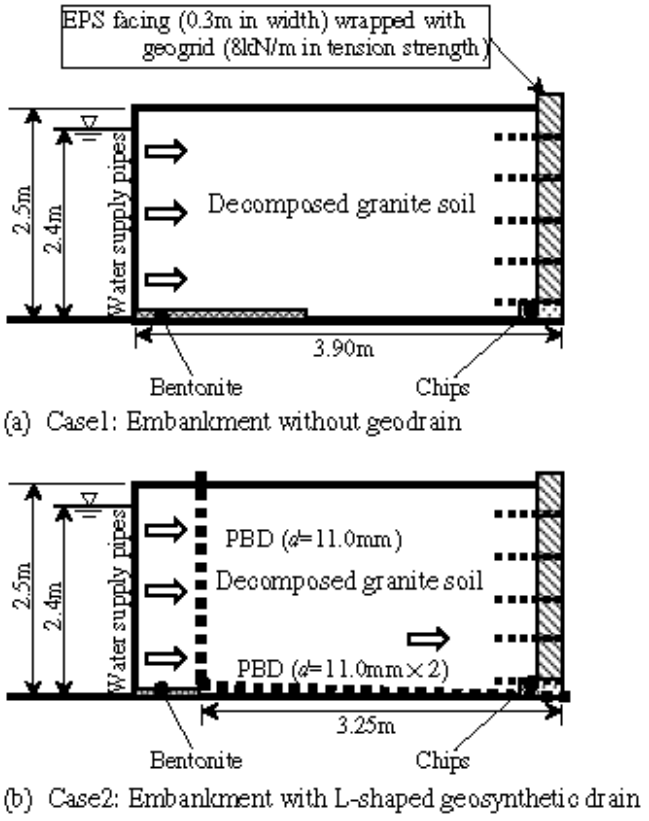


**Figure 1.** Configuration of test embankments

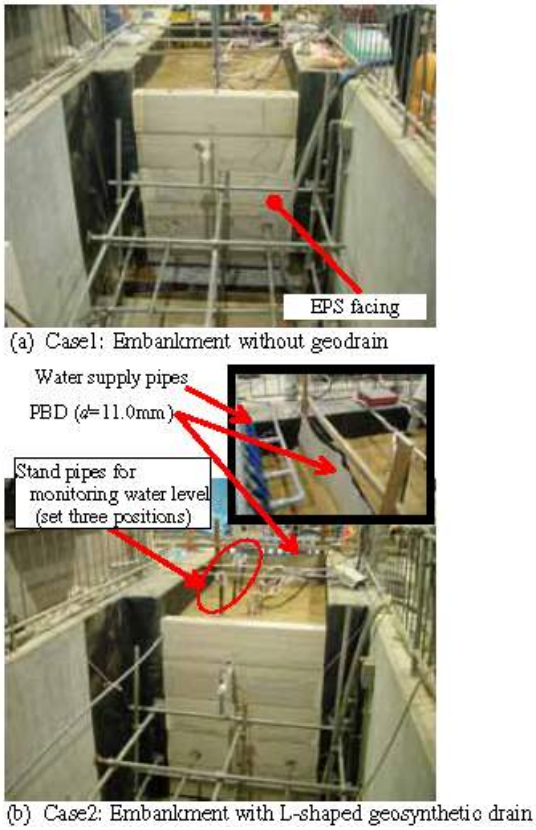


**Figure 2.** Photos of test embankments

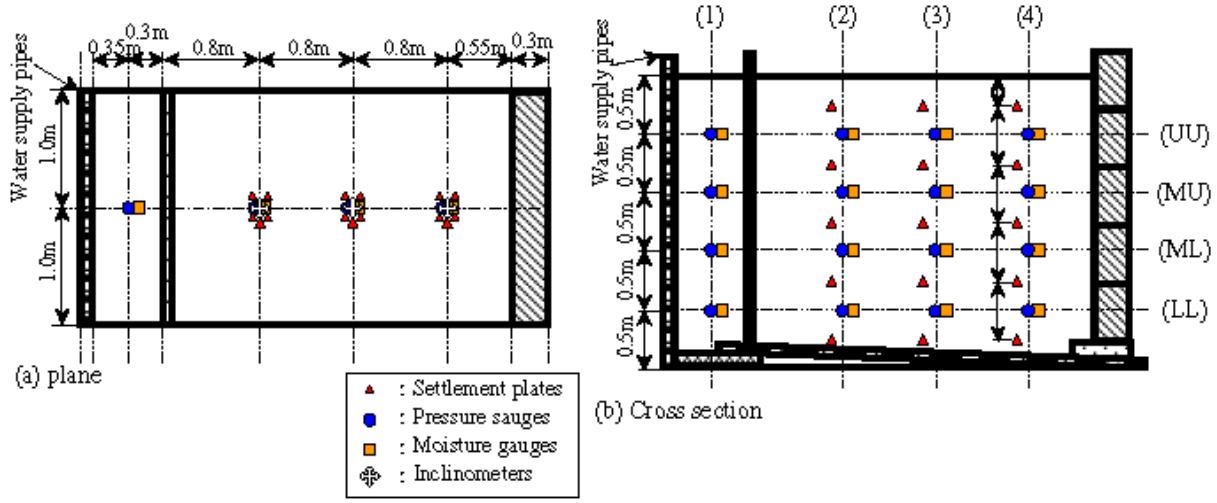


**Figure 3.** Instrumentation employed

**Seepage flow test**

In common with two test embankments, the upstream water level was raised quickly to reach a level of 2.4m from the bottom (see Figure 1). In case 2 with L-shaped geosynthetic drain, the filling and de-watering cycle was repeated twice in order to examine the response of the embankment subjected to cycles of rainfall.

Figure 4 shows the idealized flow domain in test case 2. Following the $(x,z)$ co-ordinate in Figure 4, impervious boundaries involved with $q = 0$ are considered at $z = 0$m and $z = 2.5$m at the bottom and surface of the embankment, respectively. As for seepage surface at $x = 3.6$m, the condition with $q = 0$ is satisfied when the pressure head $\psi < 0$, and $\psi = 0$ when $q < 0$.

The upstream vertical plane at $x = 0$m is the boundary to generate the water pressure varying with time. It was postulated that the water pressure rose linearly with time to reach the maximum value of $H$=2.4m. Conversely, it was assumed that in the event of dewatering, the magnitude of $H$ reduced by satisfying;

$$\frac{dH}{dt} = -\frac{Q_i(t,H)}{A} \qquad (8)$$

where $A$ represents the cross-sectional area of the water tank, and $Q_i$ denotes the rate of water inflow into the test embankment. The $Q_i$ was not a priori given so that it was calculated by iteration.

A permeability for the geosynthetic drain $k_w$ of $8.5\times10^{0}$ cm/s was employed for the numerical analysis. Conversely, the permeability of the model ground was assumed $k_s$=$8.5\times10^{-3}$ cm/s for case 1 embankment with an 85% compaction. Conversely in case 2, the value of $k_s$=$2.3\times10^{-3}$ cm/s was employed for the upstream soil with an 86% compaction, whereas the lower value of $k_s$=$6.0\times10^{-4}$ cm/s was used for the downstream soil with a 90% compaction. It should be mentioned that these permeability values are close to those measured in the laboratory. Porosity $\phi$ was fixed at the measured value of 0.35, implying that no volume change took place throughout the seepage test.

As stated earlier, the relationship between the degree of saturation and the capillary pressure exhibits a hysteretic curve against cycles of wetting and drying. An example for the relationship between capillary pressure and the degree of saturation is shown in Fig.5, in which the response at UU-1 in case 1 test is shown, together with the result of numerical simulation by means of the VG model (van Genuchten, 1980). Note that the VG model is capable of depicting the measured water retention curve well.

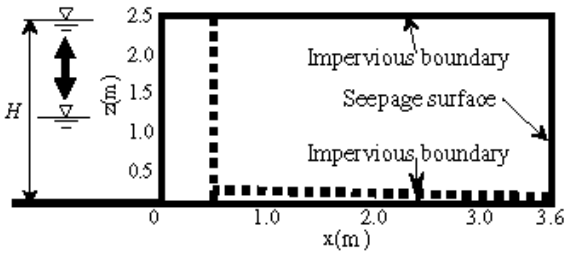


**Figure 4.** Flow domain assumed in the numerical analysis

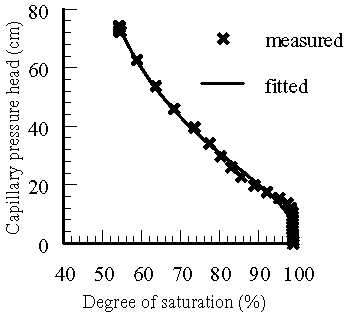


Figure 5. Water retention curves (observation vs simulation)

## DISCUSSION

### Seepage flow characteristics –observation vs. simulation

In both the cases, the vertical settlement of the test embankment was virtually zero throughout the seepage flow test, implying no volume change in these tests. The behaviour is in accordance with the assumption employed for the analysis.

The variation of degree of saturation with time is examined in Figure 6, in which the response at LL-1 and LL-4 in case 1 is examined (see Figure 3). Figure 7 shows similar observations for the variation of pore pressure head with time. The contours of pore pressure head $\psi$ since the commencement of water filling are shown in Figure 8, in which the measured water level in the standing pipes are also plotted for comparison. It should be mentioned that the numerical analysis is capable of simulating well the variations of pore pressure as well as the degree of saturation with time in the event of seepage flow.

Comparisons between the observation and the numerical simulation for case 2 test are made in Figures 9 and 10, in which the variation of $S_w$ with time at UU1 and LL-3 (see Figure 3) as well as the rate of discharge are examined, respectively. Similar to case 1, the numerical analysis was good enough for simulating not only the variations of pore pressure and the degree of saturation with time but also the rate of discharge.

Figure 11 shows the contours of $S_w$ at the elapsed time t=80hrs in case 2 test, which corresponds to a steady flow at the second stage of water filling (see Figure 10). It is obvious in this figure that the L-shaped geosynthetic drain is highly effective in reducing the downstream water level behind the vertical drain.

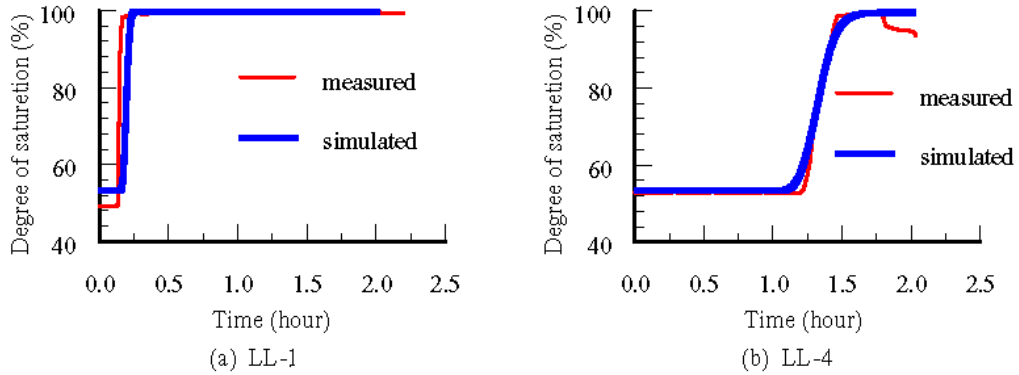


**Figure 6.** Variation of the degree of saturation with time (case 1 without L-shaped geodrain)

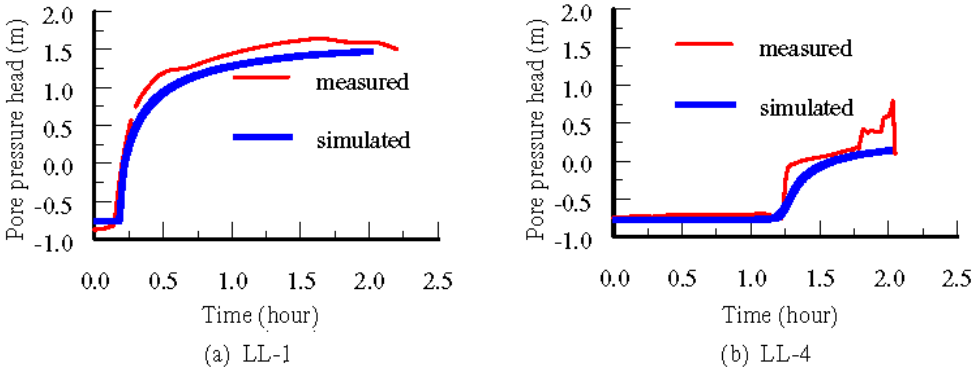


**Figure 7.** Variation of the degree of pore pressure with time (case 1 without L-shaped geodrain)

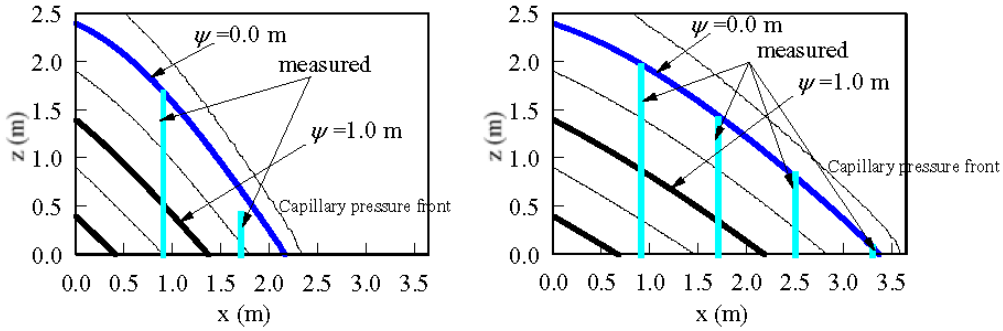


**Figure 8.** Contours of pore pressure head (case 1 without L-shaped geodrain)

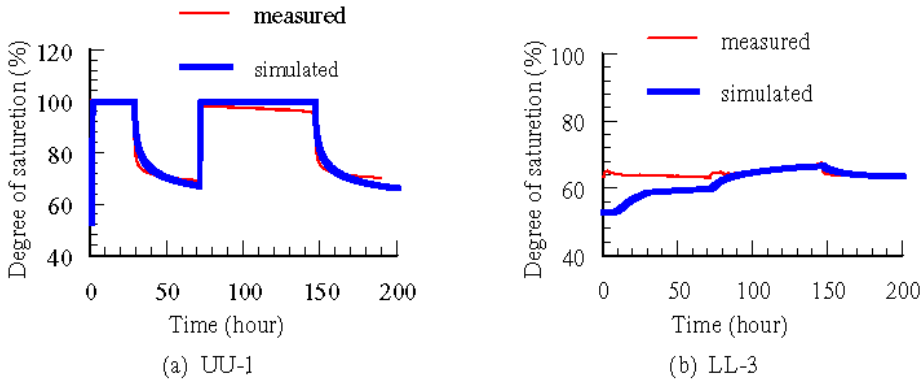


**Figure 9.** Variation of the degree of saturation with time (case 2 with L-shaped geosynthetic drain)

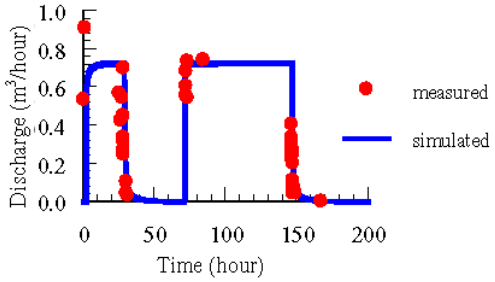


**Figure 10.** Discharge with time (case 2 with L-shaped geosynthetic drain)

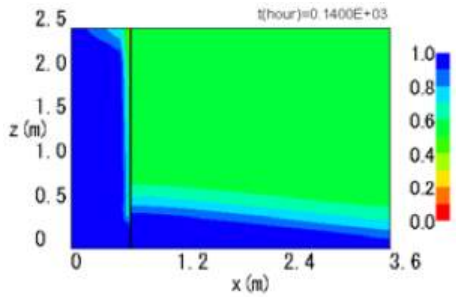


**Figure 11.** Simulation for the degree of saturation at t=140 hrs (case 2 with L-shaped geosynthetic drain)

**Deformation of test embankment**

In case 1, the embankment without the geosynthetic drain, the embankment failed after about 80mins after the start of water filling. The failure occurred as soon as the seepage front reached the chips mounted underneath the EPS block wall. As seen in Figure 12, a tension crack developed parallel to the wall at a distance of about 50cm away from the edge of the EPS wall. The failure may well be triggered by the compression failure of soil adjacent to the EPS block facing. Note also that the EPS wall reinforced with short geogrid was still effective in preventing collapse of the wall facing. More catastrophic failure subsequently took place in a manner that a sheet of thick soil fell down, resulting in complete damage of the EPS wall.

The variation of horizontal deformation with time in the case 1 embankment, together with the contours of pore pressure head is shown in Figure 13. On water filling, the upstream soil at the surface deformed by about 13mm towards the wall, whereas the other part of the embankment exhibited no deformation at all (refer to the instant at t=10min). As the seepage flow gradually progressed towards the wall, the deformation also propagated towards the downstream possibly due to the increase in water pressure behind the embankment at $x$ = 0m. At 78 mins after the filling (i.e., a few minutes before the collapse), the wall was pushed away by about 12mm at the middle and upper measuring points. The amount of displacement of the wall virtually coincided with those of three inclinometers at the corresponding level, which in turn suggests no resistance of the wall against the earth pressure. Conversely, the need for a rigid facing is strongly suggested in order to resist against the increase in earth pressure induced by the water pressure at the other end of the embankment.

In case 2, the embankment with the geosynthetic drain, the embankment showed no sign of large deformation as examined over a period of one week (see Figure 10). As stated earlier, the L-shaped geosynthetic drain was effective in reducing the downstream water level. As it can be seen in Figure 14, the water discharged as much as 0.7m$^3$ per hour from the tip of the bottom geosynthetic drain (see Figure 10).

The response of horizontal deformation in case 2 embankment, together with the contours of pore pressure head is shown in Figure 15. A trend was obvious for the horizontal deformation that the embankment deformed towards the wall and away from the wall in a synchronized manner with the filling and dewatering, respectively. However, the amount of the overall deformation was insignificant as compared to the case 1, suggesting no onset of collapse. It should be noted that the wall displacement was less than 2mm at the upper part. The efficiency of the L-shaped geosynthetic drain in reducing significantly the deformation of the protected region of the embankment is well demonstrated in these tests.

(a) First collapse

(b) Subsequent collapse

**Figure 12.** Collapse of case 1 embankment

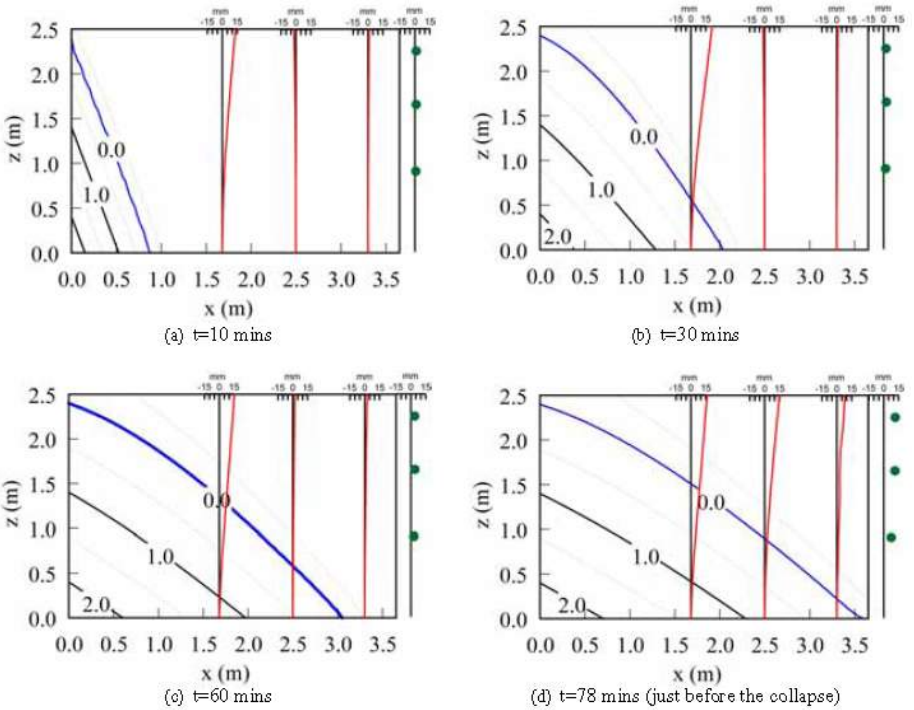


**Figure 13.** Horizontal deformation with contours of pore pressure head (case 1 without L-shaped geodrain)

**Figure 14.** Discharge of water from the tip of geosynthetic drain

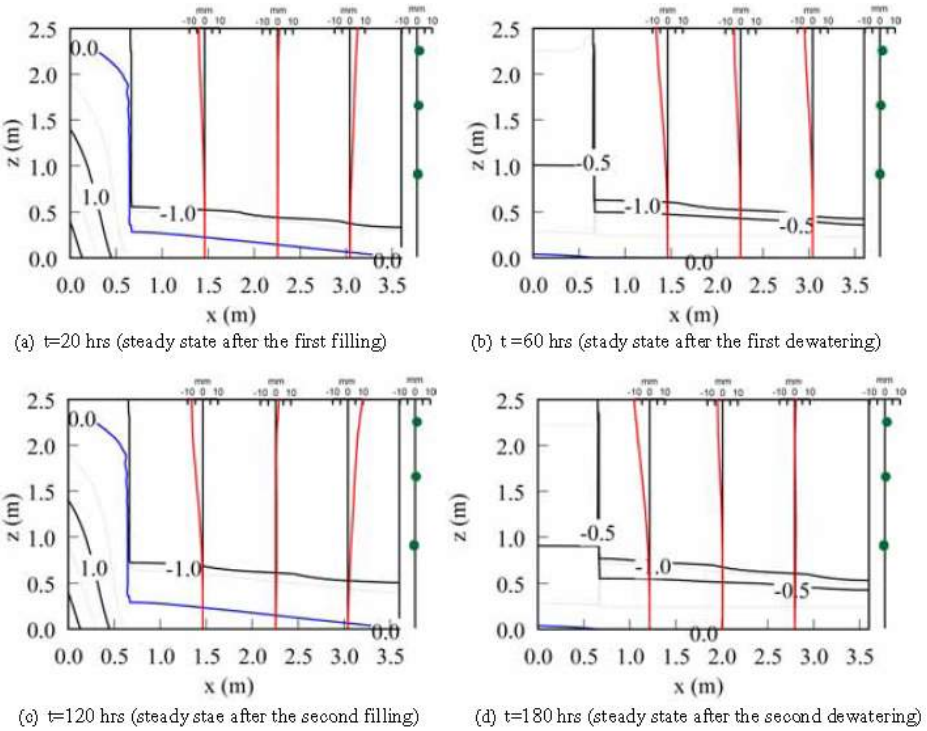


**Figure 15.** Horizontal deformation with contours of pore pressure head (case 2 with L-shaped geosynthetic drain)

## CONCLUSIONS

The concept of L-shaped geosynthetic drain is to prevent seepage flow into the embankment, and to avoid accumulation of water behind the embankment. In this paper, it was successfully demonstrated in the seepage flow test in full-scale embankment of a compacted decomposed granite soil that the L-shaped geosynthetic drain was effective in reducing significantly the water level as well as the soil deformation of the protected zone against the attack of seepage flow from the back. It was also demonstrated that the numerical analysis is capable of simulating many aspects of the seepage characteristics in well-compacted unsaturated ground such as the variations of soil suction and capillary pressure with time. When the L-shaped geosynthetic drain was not employed, the test embankment failed as soon as the seepage flow reached to the wall. On collapse, the flexible EPS facing was pushed away by a considerable amount of 12mm.The failure may have been attributed to the compression failure of soil adjacent to at the facing involved with a loss of matrix suction. Therefore, the need for a rigid facing is strongly suggested in order to resist against the increase in earth pressure induced by the accumulated water pressure behind the embankment.

## ACKNOWLEDGEMENTS

The research was supported by research grant-in-aid No. 19360214 from the Ministry of Education and Science in Japan. The authors are grateful to Messes T. Iwasaki (Soil Consultants Co. Ltd.), T. Hongo (Geo-research Institute), and J. Mitsui for their help in performing the seepage flow tests.

## REFERENCES

Hara, K. Mitsui, J., Kawai, K., Shibuya, S., Hongoh, T. & Lohani, T.N. 2007. Evaluating in-plane hydraulic conductivity of non-woven geotextile and plastic drain by laboratory test, Proc. of the 5th International Symposium on Earth Reinforcement, New Horizons in Earth Reinforcement, pp.273-279.

Hara, K., Mitsui, J., Mitsumune, J., Chae, J.G. and Shibuya, S. 2008. In-soil hydraulic transmissivity of geosynthetic drains in the laboratory, Proc. of the 4th Asian Regional Conference on Geosynthetics, Shanhai, (in press).

Luckner, L., van Genuchtn, M.Th. and Nielsen, D.R. 1989. A Consistent Set of Parametric Models for the Subsurface, Water Resources Research, Vol.25, pp.2187-2193.

Maulem, Y. 1976. A new model for predicting the hydraulic conductivity of unsaturated porous media, Water Resources Research, Vol.12, pp.513-522.

Richards, L. A. 1931. Capillary Conduction of Liquids through Porous Mediums, Physics, 1, pp.318-333.

Saito, M. Shibuya, S. Mitsui, J. & Hara, K. 2008. L-shaped geodrain in embankment −model test and numerical simulation−, Proc. of the 4th Asian Regional Conference on Geosynthetics, (in press).

Scott, P. S., Farquhar, G. J. and Kouwen, N. 1983. Hysteretic Effects on Net Infiltration, pp.163-170, In Advances in Infiltration, Am. Soc. Agric. Eng., St. Joseph, MI.

Shibuya, S. Kawaguchi, T. & Chae, J. 2007. Failure of Reinforced Earth as Attacked by Typhoon No.23 in 2004, Soils and Foundations, 47-1, pp.153-160.

Shibuya, S. Saito, M. Hara, K. & Mitsui, J. 2008. Proposal of L-shaped geodrain for preventing seepage flow into embankment using Geosynthetics. 43th Geotechnical Research Meeting, The Japanese Geotechnical Society (in press).

van Genuchten, M. T. 1980. A closed-form equation for predicting the hydraulic conductivity of unsaturated soils, Soil Science Society American Journal, Vol.44, pp.892-898.